34. M. Brandon and J. Vance, *Am. J. Sci.* **292**, 565 (1992).
35. Other factors that must be considered when reconstructing the long-term mass balance within the subduction complex include the oblique component of relative plate motion (Fig. 1), which may result in lateral material transport along north-south–trending strike-slip faults (*12*) and variable sediment input to the accretionary wedge due to the presence of large sedimentary fans offshore Washington and northern Oregon.
36. C. Goldfinger *et al.*, *Geology* **20**, 141 (1992).
37. K. Werner *et al.*, *Tectonics* **10**, 948 (1991).
38. M. Guffanti and C. S. Weaver, *J. Geophys. Res.* **93**, 6513 (1988).
39. D. Sherrod and J. Smith, *ibid.* **95**, 19465 (1990).
40. M. Guffanti *et al.*, *ibid.*, p. 19453; S. Hughes, *ibid.*, p. 19623.
41. C. DeMets *et al.*, *Geophys. J. Int.* **101**, 425 (1990).
42. We thank the many people who participated in the permitting, data acquisition, and processing phases of these experiments. Comments from M. Fisher, S. Guest, A. Jones, K. Rohr, and R. Wells greatly improved the manuscript. This work was supported by grants from NSF (OCE-8900962 and EAR-8905189 to A.M.T.) and by the U.S. Geological Survey (USGS) internal and external National Earthquake Hazards Reduction Program. Seismic instrumentation was provided by the USGS, the University of Texas at Austin, the Geological Survey of Canada, Stanford University, and the NSF IRIS/PASSCAL program. This is Geological Survey of Canada contribution number 21594.

RESEARCH ARTICLE

A Designed Peptide Ligase for Total Synthesis of Ribonuclease A with Unnatural Catalytic Residues

David Y. Jackson,* John Burnier, Clifford Quan, Mark Stanley, Jeffrey Tom, James A. Wells†

An engineered variant of subtilisin BPN′, termed subtiligase, which efficiently ligates esterified peptides in aqueous solution, was used for the complete synthesis of ribonuclease (RNase) A that contains unnatural catalytic residues. Fully active RNase A (124 residues long) was produced in milligram quantities by stepwise ligation of six esterified peptide fragments (each 12 to 30 residues long) at yields averaging 70 percent per ligation. Variants of RNase A were produced in which the catalytic histidines at positions 12 and 119 were substituted with the unnatural amino acid 4-fluorohistidine, which has a pK_a of 3.5 compared to 6.8 for histidine. Large changes in the profile of the pH as it affects rate occurred for the single and double mutants with surprisingly little change in the k_{cat} for either the RNA cleavage or hydrolysis steps. The data indicate that these imidazoles function as general acids and bases, but that the proton transfer steps are not rate-limiting when the imidazoles are present in their correct protonation states. These studies indicate the potential of subtiligase for the blockwise synthesis of large proteins.

Engineering proteins is usually limited to the application of mutagenesis and recombinant expression technologies. The ability to probe and alter protein function would be greatly expanded by generic methods to incorporate unnatural amino acids or other structures, which would allow much greater diversity and precision in protein design. However, chemical synthesis has largely been restricted to small peptides (typically less than 40 residues in length) because of the accumulation of side products that complicate product purification and decrease yields (*1*, *2*). Alternatively, coupling synthetic peptide fragments by selective chemical (*3*–*6*) or enzymatic methods (*7*–*11*) suggests that routine synthesis of proteins more than 100 residues long in high purity and good yield may soon be within reach.

Progress has been made in engineering the bacterial serine protease, subtilisin BPN′, for catalyzing peptide bond formation in aqueous solution (*9*–*11*). The most efficient variant (*11*), termed subtiligase, is a double mutant in which the catalytic Ser^{221} is converted to Cys, and Pro^{225} is mutated to Ala (S221C and P225A) (*12*). The S221C mutation increases the aminolysis to hydrolysis ratio of tetrapeptide esters (*9*, *13*) while the P225A mutation improves catalytic activity by reducing steric crowding in the active site caused by S221C. The k_{cat} value for subtiligase catalyzed aminolysis of a good peptide ester is comparable to the hydrolysis of analogous amide substrate by wild-type subtilisin (20 s^{-1} compared to 50 s^{-1}). Although this enzyme showed promise in single couplings of short peptide esters (*11*), it had not been shown to be useful for sequential couplings with long peptides.

We now describe a practical coupling and deprotection strategy that allows subtiligase to be used for the blockwise assembly of proteins. For our model synthetic protein we chose ribonuclease (RNase) A, a 124-residue enzyme, because of its interesting catalytic mechanism (*14*) and established crystal (*15*) and solution structures (*16*). The enzyme can be refolded (*17*, *18*) and easily assayed (*19*, *20*). Furthermore, RNase A has been synthesized earlier (*5*, *21*), albeit in low yield and moderate purity. The blockwise enzymatic synthesis of RNase A allowed us to produce the enzyme in higher yield and purity. As a result we were able to incorporate unnatural catalytic residues that alter the catalytic properties so that the enzyme mechanism could be probed in more detail that was not possible with conventional site-directed mutagenesis.

Synthesis of RNase A and variants containing 4-fluorohistidine. The strategy for protein synthesis with subtiligase (Fig. 1) starts with preparation of a fully deprotected peptide (the acceptor) that corresponds to the COOH-terminal fragment of the desired protein. The next most NH_2-terminal fragment (the donor) is esterified with glycolate-phenylalanyl amide (glc-F-NH_2) on the COOH-terminus. This ester efficiently acylates subtiligase because the enzyme has a preference for esters containing the glc-F-NH_2 leaving group (*11*). The donor fragment also contains an isonicotinyl (iNOC) protecting group (*22*) on its NH_2-terminus to prevent self ligation (Fig. 1). The iNOC group can be incorporated at the last step of solid phase peptide synthesis and is stable to anhydrous hydrofluoric acid, which is used to deprotect side chains and cleave peptides from the solid phase resin. After each ligation the iNOC group can be removed from the peptide under mild reducing conditions (Zn(s) and acetic acid) to generate the free NH_2-terminus for subsequent ligations.

We divided RNase A into six peptide fragments (Table 1) based on the substrate specificity of subtiligase (*11*, *23*). Subtiligase is efficient with large and hydrophobic P1 donor substrates and inefficient with negatively charged residues or Pro at P1′ (*24*). The peptides were synthesized (*25*) and ligated together in a sequential manner (*26*). The average yield was 66 percent per coupling step and 86 percent per deprotection step.

D. Y. Jackson and J. A. Wells are in the Department of Protein Engineering and J. Burnier, C. Quan, M. Stanley, and J. Tom are in the Department of Bioorganic Chemistry, Genentech, Inc., 460 Point San Bruno Boulevard, South San Francisco, CA 94080, USA.

*Present address: Department of Bioorganic Chemistry, Genentech, Inc., San Francisco, CA 94080, USA.
†To whom correspondence should be addressed.

High-performance liquid chromatography (HPLC) of a typical ligation reaction showed that the only detectable side products were those resulting from hydrolysis of the glc-F-NH_2 ester (Fig. 2A). The reduced full-length RNase A was oxidized and refolded by treatment with protein disulfide isomerase as described (*18*). The final product (~3 mg) was purified by reversed phase HPLC with a yield of 54 percent based on integration of the active peak (Table 1). The synthetic RNase A was more than 98 percent pure as assessed by SDS–polyacrylamide gel electrophoresis (SDS-PAGE) (Fig. 2B), and its mass of 13,680 daltons (Table 1) was identical to that of commercial RNase A (Sigma) as determined by electrospray ionization mass spectrometry; no other impurities were detected. Moreover, the synthetic RNase A catalyzed the hydrolysis of 2′,3′-cyclic cytidine monophosphate (CMP) with a k_{cat} of 3.3 ± 0.2 s^{-1} and K_m of 44 ± 3 μM, values that are in close agreement with those reported (k_{cat} of 3.3 s^{-1} and K_m of 42 μM) (*20*).

Three variants of RNase A (Table 2) were prepared in which the two active site histidines, His^{12} and His^{119}, were replaced singly or together with L-4-fluorohistidine (fHis). This analog is isosteric with L-histidine but has a pK_a that is reduced from 6.8 to 3.5 (*27*). Fluorohistidine was synthesized (*27*), suitably protected (*28*), and incorporated into synthetic peptides. The RNase variants containing fHis were prepared from seven peptide fragments, all of which were identical to those for wild-type RNase, except for the COOH-terminal fragment that was divided into two smaller fragments to simplify the incorporation of fHis at position 119. The average yield for the six combined coupling and deprotection steps (73 percent) was greater than that for synthesis of the wild type (56 percent) because we found that HPLC purification after each iNOC deprotection was unnecessary. Mass spectrometry confirmed the masses of the intermediate and final products at each ligation step (Table 2). The final products were refolded (*18*) and were more than 98 percent pure as determined by SDS-PAGE (Fig. 2B).

The pH-rate profiles of RNase A and 4-fluorohistidine variants. The hydrolysis of RNA by RNase A takes place in two steps, namely cleavage followed by hydrolysis (*14, 15, 29–31*). In the first step (Fig. 3A), His^{12} in its neutral form is believed to deprotonate the 2′-hydroxyl for attack on the phosphate to form a 2′,3′-cyclic phosphate intermediate. In its protonated form His^{119} is thought to facilitate the reaction by donating a proton to the 5′-oxygen leaving group (*14, 15*) or to one of the phosphate oxygens (*30*), which would produce a phosphorane intermediate in route to the cleaved product. Thus, the acidic and basic inflection points in the profiles of the pH as it affects rate (pH-rate) for cleavage of RNA substrates result from His^{12} and His^{119} serving as a general base and acid, respectively (Fig. 3B).

The incorporation of fHis into RNase caused large changes in the pH-rate profile for cleavage of uridyl-3′,5′-adenosine (Fig. 3B) that are consistent with the proposed mechanism (Fig. 3A). For example, the variant in which His^{12} was converted to fHis (H12fH) had a broadened pH-rate profile with about the same basic inflection point, but an acidic inflection point that was 2 pH units lower. This was expected from the mechanism above because $fHis^{12}$ remains in its active basic state at much lower pH. In contrast, the H119fH variant was virtually inactive at any pH. This can be explained because the pK_a of fHis at 119 is now lower than His^{12}; therefore at no pH will both imidazole side chains be in their active protonation states. Finally, the double mutant (H12fH/H119fH) has a pH-rate profile similar to wild type, but shifted down 2 pH units to reflect the lower pK_a for the two fHis side chains. Thus, lowering the pK_a of the imidazole at position 12 along with that at position 119 restores the proper relative protonation states, neutral for 12 and pro-

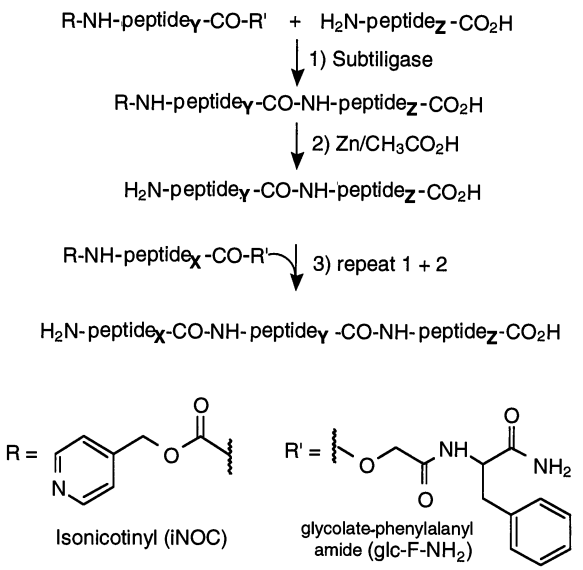

Fig. 1. General strategy for synthesizing proteins with subtiligase. Donor peptides (left) were protected on the α-amine with iNOC and esterified on the α-carboxylate with glycolate-phenylalanyl amide. The acceptor peptide (right) was fully deprotected. In step 1, the donor and acceptor peptides, lacking side-chain protecting groups, were ligated in aqueous solution with subtiligase. The ester of the donor peptide was attacked by subtiligase to produce a thiol-acyl enzyme intermediate. The α-amine of the acceptor peptide attacked the thiol-acyl bond on subtiligase to regenerate the free enzyme. In step 2, the iNOC group was removed to prepare the product as the acceptor peptide for the next ligation step. Steps 1 and 2 were repeated until full-length material was obtained. The synthesis proceeded from the most COOH-terminal fragment toward the most NH_2-terminal fragment-like standard solid phase peptide synthesis (1) except that peptide fragments were coupled instead of single amino acids.

Table 1. Summary of yields for the blockwise synthesis of wild-type RNase A. Peptide fragments (**1–6**) were synthesized using butoxycarbonyl (BOC) chemistry to have the following amino acid sequences: **1**, iNOC-HN-KETAAAKFERQHMDSSTSAA-CO-R′ (residues 1–20); **2**, iNOC-HN-SSSNYCNQMMKSRNLTKDRCKPVNTFVHESL-CO-R′ (residues 21–51); **3**, iNOC-HN-ADVQAVCSQKNV-CO-R′ (residues 52–63); **4**, iNOC-HN-ACKNGQTNCYQSY-CO-R′ (residues 64–76); **5**, iNOC-HN-STMSITDCRE TGSSK YPNCAY-CO-R′ (residues 77–97); **6**, H_2N-KTTQANKHIIVACEGNPYVPVHFDASV-CO_2H (residues 98–124) where R′ is glycolate-phenylalanyl amide (see Fig. 1). The yields are based on the molar ratio of isolated product to the COOH-terminal substrate which was the limiting reagent in each case. The average yield per ligation is 66 percent and per deprotection is 86 percent.

Step	Fragment	Reaction	Yield (%)	Mass	
				Calc.	Found
1	**5 + 6**	Coupling	63	5370.7	5368.9
	iNOC-**5–6**	Deprotection	91	5233.9	5234.4
2	**4 + 5–6**	Coupling	76	6832.0	6831.5
	iNOC-**4–6**	Deprotection	87	6695.2	6695.0
3	**3 + 4–6**	Coupling	68	8075.4	8075.0
	iNOC-**3–6**	Deprotection	81	7939.4	7938.5
4	**2 + 3–6**	Coupling	55	11675.6	11676
	iNOC-**2–6**	Deprotection	83	11539.4	11538
5	**1 + 2–6**	Coupling	67	13824.0	13824
	iNOC-**1–6**	Deprotection	90	13688.0	13687
6	**1–6**	Refolding	54	13679.8	13680

tonated for 119. Findlay *et al.* (*31*) have shown that the optimal pH for RNase A activity is shifted nearly two units when the enzyme is assayed in 1:1 mixture of dioxane and water. The addition of organic solvent lowers the pK_a of the imidazole side chains and results in an analogous shift in the pH activity profile to that seen for the double mutant.

In the second and slower step of the reaction (Fig. 4A), the enzyme catalyzes the hydrolysis of the 2′,3′-cyclic phosphate intermediate. Here the catalytic roles of His^{12} and His^{119} are thought to be reversed (*14*): A neutral His^{119} acts as a general base to deprotonate a water molecule for attack on the 2′,3′-cyclic uridine monophosphate (UMP) while the protonated form of His^{12} acts as an acid by protonating the 2′ oxygen. Thus, the pH-rate profile for hydrolysis of 2′,3′-cyclic UMP by synthetic wild-type RNase A is bell-shaped (Fig. 4B) and is the same as that reported for commercial RNase A. The acidic limb is believed to reflect the need for a neutral His^{119} and the basic limb reflects the requirement for the protonated form of His^{12}.

Substitutions of fHis into positions 12 and 119 again caused large changes in the pH-rate profiles, some of which were expected but some were not. For example, the inflection points in the pH-rate profile for the H12fH variant were surprisingly close to those for wild-type RNase A (Fig. 4B) and the catalytic activity was only six times lower. This indicates that His^{12} may not be responsible for the basic limb of the pH profile, and that His^{12} probably plays a minor catalytic role in this step. The single H119fH substitution caused a lowering of the acidic limb of the pH-rate profile by about 2 pH units for step 2, but an unexpected shift in the basic limb as well (Fig. 4B). The double mutant and the single H119fH variant had similar inflection points further suggesting that the protonation state of His^{12} is not critical.

These data are consistent with His^{119} acting as a general base in step 2, but do not support the role of His^{12} as an acid. This raises the questions: what is responsible for the basic limb of the pH-rate profile for step 2, and why do both limbs shift for the H119fH variant? It is conceivable that the basic limb is caused by a protonated form of Lys^{41}, which is nearby and is believed to stabilize the negatively charged phosphate by way of an electrostatic interaction (Fig. 5). Mutations at Lys^{41} profoundly affect catalysis (*32*). Furthermore, hydrolysis of the cyclic phosphate may occur by the 2′ oxygen receiving a proton directly from solvent. Thus, for the H119fH variant, it is possible that the acidic limb reflects the need for a neutral imidazole at position 119 and the basic limb results from the reduction in the concentration of protons in solution. Additional experiments are needed to clarify these possibilities.

The interpretation of protonation states of residues in the active sites of enzymes based on pH-rate profiles can present problems (*33*) because among others, the microenvironment of the enzyme can affect the pK_a of residues. However, the micro environment of the active site for the wild-type or fHis variants should be similar, and therefore should affect the pK_a's of either in a similar fashion. Changes in the pH-rate profile observed at low pH probably do not reflect large structural changes because RNase A is stable to acid denaturation down to pH 3 (*14*). In addition, it is unlikely that the fHis substitutions alter the structure of the RNase because fluorohistidine is isosteric with histidine. In fact, a shortened version of the ribonuclease S–peptide (residues 1–15) has been previously synthesized containing (L)-4-fluorohistidine at position 12 and reassociated with RNase S–protein (residues 21–124) to form a noncovalent RNase S complex. Crystallographic studies of this mutant complex showed that the overall backbone structure and side-chain configuration of the 4-fluorohistidine mutant was unchanged relative to wild-type RNase S (*35*).

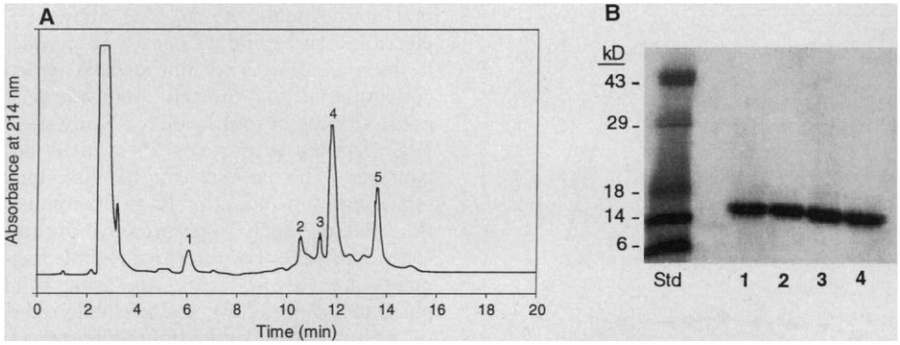

Fig. 2. (**A**) Analytical HPLC of the ligation of fragments **5** and **6** containing RNase A residues 77–97 and 98–124, respectively (Table 1). A solution of fragment **5** (3 mg in 200 μl of DMF) was added to fragment **6** (10 mg) and subtiligase (0.2 mg) in 2 ml of 100 mM tricine, pH 8. The mixture was reacted for 1 hour at 25°C and subjected to HPLC (20 to 50 percent CH_3CN for 20 minutes at 1.5 ml/min). All peaks were identified by mass spectrometry. Peak 1 was glycolate-phenylalanyl amide generated from aminolysis and hydrolysis of fragment **5**: peak 2 was hydrolyzed fragment **5**; peak 3 was unreacted fragment **5**; peak 4 was unreacted excess acceptor peptide **6**; and peak 5 was the desired ligation product (iNOC-fragment **5–6**). (**B**) SDS–polyacrylamide gel electrophoresis (16 percent acrylamide) showing synthetic wild-type and mutant RNase A (lanes 1 to 4). Lane 1, wild-type RNase A; lane 2, H12fH RNase A; lane 3, H119fH RNase A; lane 4, the double mutant. Each lane contained about 5 μg of protein.

Table 2. Summary of yields for the blockwise synthesis of mutants of 4-fluorohistidine RNase A. The ligation junctions are the same as those used to construct wild-type RNase (Table 1) except that the COOH-terminal fragment (98–124) was divided in two (residues 98–115 and 116–124), which facilitated incorporation of (L)-4-fluorohistidine (**fH**) at position 119. Fragment peptides (**1–7**) had the following amino acid sequences: **1**, iNOC-HN-KETAAAKFERQ(**fH**)MDSSTSAA-CO-R′ (residues 1–20); **2**, iNOC-HN-SSSNYCNQMMKSRNLTKDRCKPVNTFVHESL-CO-R′ (residues 21–51); **3**, iNOC-HN-ADVQAVCSQ-KNV-CO-R′ (residues 52–63); **4**, iNOC-HN-ACKNGQTNCYQSY-CO-R′ (residues 64–76); **5**, iNOC-HN-STMSITDCRETG SSKYPNCAY-CO-R′ (residues 77–97); **6**, R-HN-KTTQANKHIIVACEGNPY-CO-R′ (residues 98–115); **7**, H_2N-VPV(**fH**)FDASV-CO_2H (116–124) where R′ is glycolate-phenylalanyl amide (see Fig. 1). For the single mutants, H12fH and H119fH, peptides containing histidine in place of fluorohistidine were substituted at positions 119 and 12, respectively. The yields for combined coupling and deprotection steps are based on molar ratio of isolated product compared to the COOH-terminal substrate which was the limiting reagent in each case.

Step	Reaction	Yield (%)	Mass	
			Calc.	Found
1	**6 + 7**	61	2937.4	2938.1
2	**5 + (6–7)**	77	5252.0	5252.5
3	**4 + (5–7)**	78	6713.1	6714.0
4	**3 + (4–7)**	80	7957.4	7958.2
5	**2 + (3–7)**	68	11539.4	11540
6	**1 + (2–7)**	73	13724.0	13725
7	Refolding	50	13716.0	13717 (H12fH/H119fH)
		55	13688.0	13689 (H12fH)
		55	13688.0	13689 (H119fH)

Although the pH-rate profiles were not reported, it was noted that the semisynthetic complex was devoid of catalytic activity.

We find that incorporation of fHis into full-length RNase A causes large shifts in the pH-rate profiles yet the relative catalytic rates are only slightly reduced from the wild-type enzyme. Thus reducing the pK_a's of the imidazoles by ~3 pH units does not grossly affect the ability of the enzyme substrate complex to reach either of the two transition states. This suggests the proton transfer steps are not rate-limiting assuming the imidazoles are in their proper protonation states. These data are not inconsistent with studies showing that mutation of His^{12} or His^{119} to alanine decreases activity of step 1 by 10^4 and 10^3 times, respectively (*36*). When the imidazoles are absent, proton transfer may then be a rate-limiting step because the enzyme depends on the solvent (instead of the imidazoles) as the immediate source of protons or hydroxide ions. Our data support proposals that the imidazoles function as general acids and bases in step 1 but that they deliver and accept protons before or after the transition state is reached.

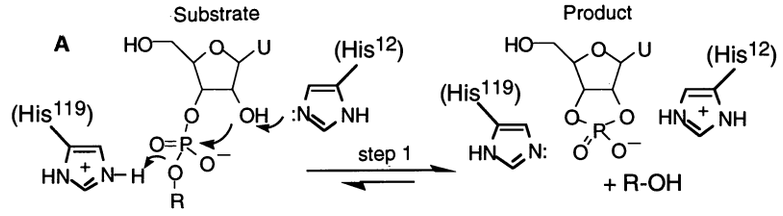

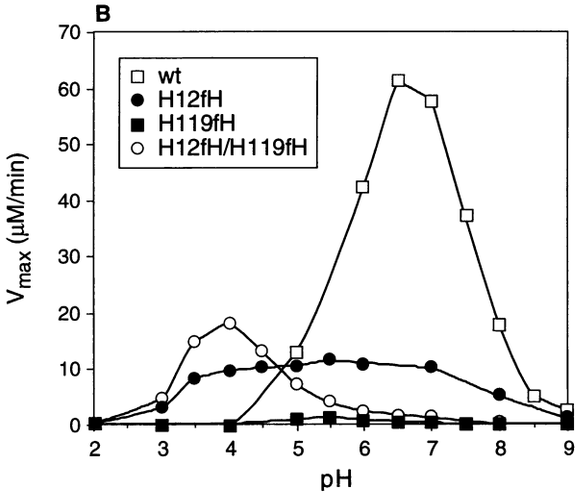

Fig. 3. (**A**) Mechanism of cleavage of the dinucleotide RNA substrate [uridyl-3′,5′-adenosine (UpA)] by RNase A (*14*). His^{12} acts as a general base whereas His^{119} acts as a general acid. (**B**) Plot of relative rate as a function of pH for cleavage of UpA. The initial rate of UpA cleavage was measured spectrophotometrically by means of an adenosine deaminase coupled assay (*19*). Assays were performed at 25°C in 100 mM citrate (pH 3 to 6) or in 100 mM tricine (pH 6.5 to 9). The relative rate at each pH was determined by addition of substrate (2 mM final) to enzyme (0.1 μM) in the appropriate buffer. The spontaneous background rate of cleavage (no enzyme) was determined at each pH and subtracted from the enzyme-catalyzed rates to yield corrected values. The products of each assay were separated by HPLC and identified by mass spectrometry.

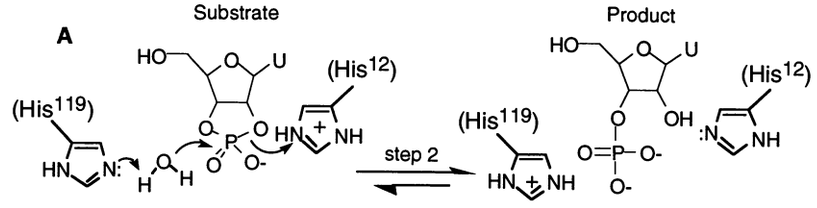

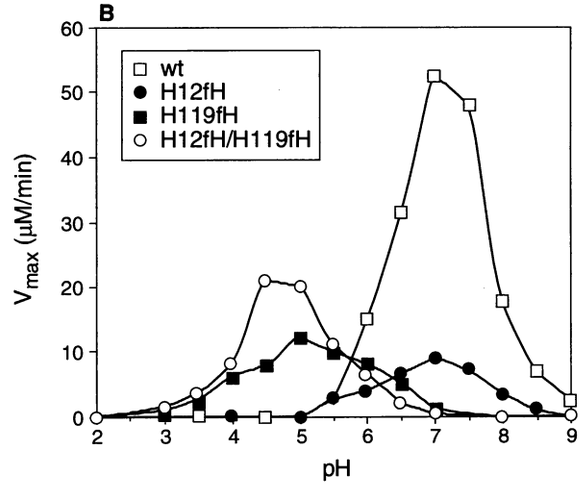

Fig. 4. (**A**) Mechanism of the hydrolysis of cyclic 2′,3′ uridine monophosphate (cyclic UMP) by wild-type and 4-fluorohistidine mutants of RNase A. The roles of the catalytic histidines are thought to be reversed relative to step 1 (Fig. 3A) with His^{12} acting as a general acid and His^{119} as a general base (*14*). (**B**) The rate of cyclic UMP hydrolysis was measured spectrophotometrically as described (*20*). Assays were performed and analyzed as in Fig. 3 except that the initial substrate and enzyme concentrations were 1 mM and 1 μM, respectively.

Use of subtiligase in peptide and protein synthesis. The incorporation of unnatural amino acids (*4*, *37*, *38*) allows the electronic and steric properties of enzymes to be altered in ways not possible when conventional site-directed mutagenesis is used. The use of subtiligase for synthesis of large peptides or proteins offers many advantages. The protein can be assembled sequentially in blocks of 10 to 30 residues thus making much larger proteins synthetically accessible. The esterified peptide fragments are easy to synthesize using solid phase techniques (*25*), and no labile esters (*4*) are introduced in the final protein product. Side chains are fully deprotected prior to ligation making the peptides more soluble in water. The peptide ligations are done in solution and each ligation intermediate is purified by HPLC; thus side products are not carried through the synthesis. Moreover, milligram quantities of product can be produced and multiple substitutions can be made in the same protein. This is in contrast to in vitro transcription/translation methods (*37*, *38*) where products are produced typically in microgram amounts and substitutions are limited in practice to a single site.

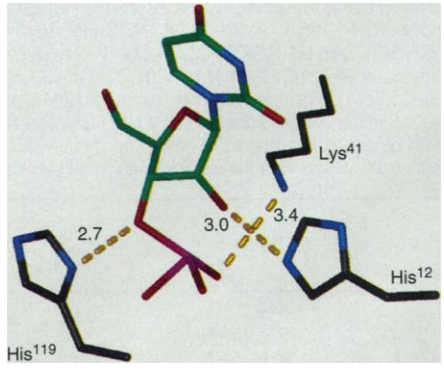

Fig. 5. Active site residues (His^{12}, His^{119}, and Lys^{41}) of RNase A complexed to a uridine vanadate transition state analog inhibitor (in grey) taken from a 1.8 Å neutron structure (*15*). The relevant distances (Å) from side chains to inhibitor are shown (dashed yellow lines).

The subtiligase synthetic technology is, however, limited to proteins that can be refolded in vitro. The size of the protein one can synthesize is limited to the ability to prepare synthetic fragments. Although the subtiligase has rather broad specificity requirements (*11*, *23*), care must be taken in designing ligation junctions to be compatible with the enzyme. The average yield per ligation is high (~75 percent); however, the overall yield for the six ligation steps was 15 percent, and after refolding was 8 percent (Table 2). Nonetheless, one can obtain synthetic RNase A in 10-mg quantities from 100 mg of starting peptide.

The subtiligase technology can be adapted to semi-synthesis of proteins; peptides have been ligated onto the NH_2-terminus of natural or recombinant proteins or protein fragments (*23*). Protein synthesis with subtiligase may allow more efficient production of proteins that are poorly expressed by recombinant means due to instability or toxicity. Finally, the efficient incorporation of synthetic amino acids into proteins greatly enhances the ability of chemists and biologists to understand existing proteins and to create new proteins with altered and useful properties.

REFERENCES AND NOTES

1. M. Bodanszky and A. Bodanszky, *The Practice of Peptide Synthesis* (Springer-Verlag, New York, 1984), vol. 21.
2. E. T. Kaiser, *Acc. Chem. Res.* **22**, 47 (1989).
3. S. B. H. Kent, *Annu. Rev. Biochem.* **57**, 957 (1988).
4. M. Schnolzer and S. B. H. Kent, *Science* **256**, 221 (1992).
5. R. Hirschmann *et al.*, *J. Am. Chem. Soc.* **91**, 502 (1969).
6. N. Fujii and H. Yajima, *J. Chem. Soc., Perkins Trans.* **1**, 789, 797, 804 (1981).
7. C. Wong, M. Schuster, P. Wang, P. Sears, *J. Am. Chem. Soc.* **115**, 5893 (1993).
8. W. Kullman, *Enzymatic Peptide Synthesis* (CRC Press, Boca Raton, FL, 1987).
9. T. Nakatsuka, T. Sasaki, E. T. Kaiser, *J. Am. Chem. Soc.* **109**, 3808 (1987).
10. Z. Wu and D. Hilvert, *ibid.* **111**, 2414 (1989).
11. L. Abrahmsen *et al.*, *Biochemistry* **30**, 4151 (1991).
12. Mutations are designated by the wild-type residue, followed by the residue's position and then the mutant residue in single-letter code. Multiple mutants are indicated by a series of single mutants separated by a slash. Abbreviations for the amino acid residues are: A, Ala; C, Cys; D, Asp; E, Glu; F, Phe; G, Gly; H, His; I, Ile; K, Lys; L, Leu; M, Met; N, Asn; P, Pro; Q, Gln; R, Arg; S, Ser; T, Thr; V, Val; W, Trp; and Y, Tyr.
13. T. C. Bruice, J. J. Bruno, W. Chou, *J. Am. Chem. Soc.* **85**, 1659 (1963); K. Neet and D. Koshland, *Proc. Natl. Acad. Sci. U.S.A.* **56**, 1606 (1966); L. Polgar and M. L. Bender, *J. Am. Chem. Soc.* **88**, 3153 (1966).
14. P. Blackburn and S. Moore, *The Enzymes* (Academic Press, New York, 1982), vol. 15.
15. R. L. Campbell and G. A. Petsko, *Biochemistry* **26**, 8579 (1987).
16. M. Rico *et al.*, *J. Biol. NMR* **1**, 283 (1991).
17. D. M. Rothwarf and H. A. Scheraga, *Biochemistry* **32**, 2671 (1993).
18. M. M. Lyles and H. F. Gilbert, *ibid.* **30**, 613 (1991).
19. P. L. Ipata and R. L. Felicioli, *FEBS Lett.* **1**, 29 (1968).
20. A. L. Fink, D. Kar, R. Kotin, *Biochemistry* **26**, 8571 (1987).
21. B. Gutte and R. B. Merrifield, *J. Biol. Chem.* **246**, 1922 (1971).
22. D. F. Veber, W. J. Paleveda, Y. C. Lee, R. Hirschmann, *J. Org. Chem.* **42**, 3286 (1977).
23. T. Chang, D. Y. Jackson, J. Burnier, J. A. Wells, *Proc. Natl. Acad. Sci. U.S.A.*, in press.
24. Protease substrates are designated NH_2-Pn. . .P2-P1-P1′-P2′. . .Pn′-COOH, where the cleaved bond is between the P1 and P1′ residues [I. Schechter and A. Berger, *Biochem. Biophys. Res. Commun.* **27**, 157 (1967)]. We have adopted the same nomenclature to describe ligation substrates, where the synthesized bond is between P1 and P1′.
25. Glycolate-activated and iNOC-protected peptides were synthesized as follows. Phenylalanyl-*p*-methylbenzhydryl amine (MBHA) resin (0.63 meq/g; Advanced ChemTech) was stirred with bromoacetic acid (5 eq) and diisopropyl carbodiimide (5 eq) for 1 hour at 25°C in dimethylacetamide (DMA) to afford the bromoacetyl derivative. The resin was washed extensively with DMA, and individual butyloxycarbonyl (BOC)-protected amino acids (3 eq, Bachem) were esterified by stirring with sodium bicarbonate (6 eq) in dimethylformamide (DMF) for 24 hours at 50°C to yield the corresponding glc-F-NH_2 resin. The aminoacetylated resin was washed with DMF and dichloromethane (CH_2Cl_2) and could be stored at room temperature for several months. The resin was placed in an automated peptide synthesizer (Applied Biosystems 430A) and the resulting peptides were elongated by standard solid phase procedures (*1*). The N-α-BOC group was removed with a solution of 45 percent trifluoroacetic acid (TFA) in CH_2Cl_2. Subsequent BOC-protected amino acids (5 eq) were first activated with benzotriazol-1-yl-oxy-tris-(dimethylamino) phosphonium hexafluorophosphate (BOP, 4 eq) and *N*-methylmorpholine (NMM, 10 eq) in DMA and coupled for 1 to 2 hours. The final *N*-α-Boc group was removed (TFA and CH_2Cl_2) and the isonicotinyl (iNOC) protecting group was introduced as described (*22*) by stirring with of 4-isonicotinyl-2-4-dinitrophenyl carbonate (3 eq) and NMM (6 eq) in DMA at 25°C for 24 hours. Cleavage and deprotection of the peptide by treatment with anhydrous hydrofluoric acid (in 5 percent anisole and 5 percent ethylmethyl sulfide) at 0°C for 1 hour produced the iNOC-protected, glc-F-NH_2-activated peptide (Fig. 1) which was purified by reversed phase C18 HPLC (CH_3CN and H_2O gradient, 0.1 percent TFA). The identity of all substrates was confirmed by mass spectrometry.
26. Ligations were performed at 25°C in ligase buffer (100 mM tricine, pH 8 freshly prepared and degassed by vacuum filtration through a 5 μm filter) containing 2 to 5 mM acceptor peptide and ~5 μM subtiligase. Three to five equivalents of lyophilized glycolate-phenylalanyl amide (glc-F-NH_2) activated donor peptide was dissolved into the solution, and the mixture was incubated for 1 to 2 hours at 25°C. The ligation reactions were monitored by analytical reversed phase C18 HPLC (CH_3CN and H_2O gradient with 0.1 percent TFA). In some cases, hydrolysis of the donor peptide precluded complete disappearance of the acceptor peptide and thus an additional 3 eq of donor glc-F-NH_2 activated peptide was added. In all cases, this was sufficient to drive ligation to completion. Isonicotinyl deprotection was performed as described (*22*) by stirring 50 mg of HCl activated zinc dust with the protected peptide in 2 ml of CH_3CO_2H for 2 hours. The zinc dust was removed by filtration, and the CH_3CO_2H was removed under reduced pressure. The product was purified by preparative C18 HPLC (CH_3CN and H_2O gradient) and fractions containing pure material were lyophilized to yield material suitable for subsequent ligation. The identity and purity of all isolated intermediates was confirmed by mass spectrometry (Sciex electrospray ionization mass spectrometer).
27. K. L. Kirk and L. A. Cohen, *J. Am. Chem. Soc.* **95**, 4619 (1973).
28. (L) 4-fluorohistidine was synthesized (*27*) and the amino group was protected with butoxycarbonyl (BOC) anhydride under standard conditions (*1*). The imidazole moiety was protected with benzyl chloromethyl ether (BOM) protecting group for histidine by standard methods [T. B. Brown and J. H. Jones, *J. Chem. Soc. Chem. Comm.* **408**, 648 (1981)]. The final protected amino acid was purified by silica gel chromatography (eluting with ethyl acetate, hexane, and 2 percent acetic acid). The solvent was evaporated and the residue was dissolved in H_2O and acetonitrile. Lyophilization afforded a white solid (free acid) suitable for solid phase peptide synthesis.
29. D. A. Usher, E. S. Erenrich, F. Eckstein, *Proc. Natl. Acad. Sci. U.S.A.* **69**, 115 (1972).
30. R. Breslow, E. Anslyn, D. Huang, *Tetrahedron* **47**, 2365 (1991); E. Anslyn and R. Breslow, *J. Am. Chem. Soc.* **111**, 4473 (1989).
31. D. Findlay, A. P. Mathias, B. R. Rabin, *Biochem. J.* **85**, 139 (1962).
32. K. Trautwein, P. Hollinger, J. Stackhouse, S. A. Benner, *FEBS Lett.* **281**, 275 (1991).
33. J. Knowles, *CRC Crit. Rev. Biochem.* **4**, 165 (1976).
34. B. M. Dunn, C. Dibello, K. L. Kirk, L. A. Cohen, I. M. Chaiken, *J. Biol. Chem.* **249**, 6295 (1974).
35. H. C. Taylor *et al.*, *J. Mol. Biol.* **149**, 313 (1981).
36. J. E. Thompson and R. T. Raines, *J. Am. Chem. Soc.* **116**, 5467 (1994).
37. C. J. Noren, S. J. Anthony-Cahill, M. C. Griffith, P. G. Schultz, *Science* **244**, 182 (1989).
38. D. Mendel *et al.*, *ibid.* **256**, 1798 (1992).

39. We thank J. Bourell, B. Gillece-Castro, K. O'Connell, L. Nuwaysir, and D. Burdick for the numerous mass spectra; M. Struble and K. Chan for peptide purification; T. Chang, K. Judice, and J. Kirsch for discussions; and the Damon Runyan–Walter Winchell Cancer Research fund for postdoctoral support (D.Y.J.).

20 April 1994; accepted 2 September 1994